NJC

RSC Publishing

PAPER

View Article Online
View Journal | View Issue

Cite this: *New J. Chem.*, 2013, **37**, 4206

Piperazine-based simple structure for selective sensing of Hg^{2+} and glutathione and construction of a logic circuit mimicking an INHIBIT gate†

Kumaresh Ghosh,*[a] Debojyoti Tarafdar,[a] Asmita Samadder[b] and Anisur Rahman Khuda-Bukhsh[b]

Received (in Montpellier, France) 29th July 2013,
Accepted 17th September 2013

DOI: 10.1039/c3nj00855j

www.rsc.org/njc

A simple chemosensor (**1**) has been designed and synthesized. The chemosensor selectively recognizes Hg^{2+} ions in THF–H_2O (3 : 1, v/v) by showing a significant increase in emission and a bluish color of the solution under exposure to UV light. Change of the fluorophore unit in **1** leads to **2**, which also shows selective sensing of Hg^{2+} under similar conditions. Furthermore, while the ensemble of **1** with Hg^{2+} selectively senses reduced glutathione (GSH) over cysteine and homocysteine, the ensemble of **2** with Hg^{2+} has been observed to be inefficient to distinguish glutathione from other biothiols. Thus probe **1** and inputs Hg^{2+} and GSH can be used to develop an INHIBIT logic gate.

Introduction

Design and synthesis of simple and easy-to-make optical chemosensors for the selective recognition of toxic metal ions has drawn much attention.[1] Among the different toxic metal ions, mercury is considered to be dangerous. Its accumulation in a low concentration in the human body causes a wide variety of diseases, such as prenatal brain damage, serious cognitive disorders, and Minamata disease.[2] The toxicity of mercury in living systems is attributed to the measurable affinities of thiol group containing proteins and enzymes, which result in the malfunctioning of living cells.[3] Therefore, the detection and sensing of this toxic metal ion is a sensible issue to chemists. Of the different techniques, fluorescence is of considerable interest due to its simplicity, high sensitivity and real-time detection. To date, many fluorescent probes for Hg^{2+} ions have been reported.[4,5] The majority of the probes for Hg^{2+} are 'turn-off'[6] because Hg^{2+} produces mostly a CHEQ (chelation-enhanced quenching) effect, presumably because of the large spin–orbit coupling constant value.[7] The design of fluorescence 'turn-on' type sensors upon mercury binding is thus a challenging issue and only a few fluorescence 'turn-on' sensors for mercury have been reported.[8]

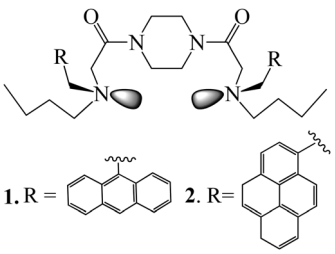

Scheme 1 Structures of **1** and **2**.

In this account, we report the simple and easy-to-make PET (photoinduced electron transfer) systems **1** and **2** (Scheme 1), which serve dual purposes: (i) the recognition of Hg^{2+} ions in THF–H_2O (3 : 1, v/v) and (ii) acting as an INHIBIT logic gate in reporting the selective detection of glutathione over cysteine and homocysteine. Biothiols such as cysteine, homocysteine and glutathione play crucial roles in biological systems and therefore, their recognition and sensing draws attention.[9] It is mentionable that glutathione (GSH) is the most abundant cellular thiol compound that plays a central role in combating oxidative stress in cells.[10] Abnormal levels of GSH are associated with a number of diseases, including cancer, AIDS, Alzheimer's and cardiovascular disease.[11] Thus the measurement of GSH in physiological media has been considered an essential factor in the diagnosis of these diseases. Several common strategies are known to detect GSH, such as electrochemical assays,[12] high-performance liquid chromatography (HPLC),[13] mass spectrometry,[14] fluorescence spectrometry[15] and enzymatic methods.[16] Among these reported detection methods, fluorescent sensing has attracted considerable attention due to its simple operation and high sensitivity.

[a] *Department of Chemistry, University of Kalyani, Kalyani-741235, India. E-mail: ghosh_k2003@yahoo.co.in; Fax: +91 3325828282; Tel: +91 3325828750*
[b] *Department of Zoology, University of Kalyani, Kalyani-741235, India*

† Electronic supplementary information (ESI) available: Figures showing the fluorescence and UV-vis titrations of **1** and **2** with various metal ions, Job plot, binding curves, IR comparison, selectivity test, detection sensitivity, change in emission of **1** and **2** upon titration with biothiols, MTT assay, ^{1}H NMR, ^{13}C NMR and mass spectra of **1** and **2**. See DOI: 10.1039/c3nj00855j

Results and discussion

Synthesis of chemosensors **1** and **2** was achieved according to Scheme 2. Piperazine on reaction with chloroacetyl chloride in the presence of Et_3N in dry CH_2Cl_2 gave dichloroamide **3** (Scheme 2a). On the other hand, the anthracene coupled amine **5**, obtained from 9-anthraldehyde *via* Schiff base formation followed by reduction with $NaBH_4$ was refluxed with compound **3** in the presence of anhydrous K_2CO_3 in dry CH_3CN to give the desired compound **1** (Scheme 2b). In a similar way, the pyrene coupled amine **7** obtained from pyrene aldehyde through a series of reactions as shown in Scheme 2c was treated with **3** to afford compound **2**. Both compounds **1** and **2** are soluble in $CHCl_3$, CH_2Cl_2, DMSO, THF and DMF. They are partially soluble in CH_3CN and CH_3OH. All the compounds were characterised spectroscopically.

The metal ion binding properties of **1** towards Hg^{2+}, Cu^{2+}, Cd^{2+}, Fe^{2+}, Mg^{2+}, Co^{2+}, Ni^{2+}, Zn^{2+}, Ag^{+} and Pb^{2+} (taken as their perchlorate salts; **caution**: perchlorate salts are sometimes an explosive hazard[17]) were initially pursued in THF. First, we investigated the affinity of chemosensor **1** towards Hg^{2+} ions by monitoring the emission upon gradual addition of $Hg(ClO_4)_2$ to the solution of compound **1** ($c = 2.5 \times 10^{-5}$ M) in THF. As can be seen from Fig. 1, upon excitation at 370 nm receptor **1** exhibited a characteristic weak broad emission centered at 412 nm. While titrating, the emission at 412 nm increased dramatically upon the incremental addition of only 1.5 equiv. of Hg^{2+} ions. During the titration, the emission intensity at 412 nm progressively increased with red shift ($\Delta\lambda$ = 10 nm). Upon interaction with Hg^{2+} ions, the solution of **1** turned a bluish color when observed under exposure to UV irradiation (inset of Fig. 1). The notable increase in the emission of **1** in the presence of Hg^{2+} ions is attributed to the strong coordination of Hg^{2+} by tertiary amine nitrogens, which prevents photo-induced electron transfer (PET) from the binding sites to the excited state of anthracene. However, among the other cations, only Cu^{2+} and Pb^{2+} weakly perturbed the emission (Fig. 2).

In order to observe the sensing behaviour of **1** towards Hg^{2+} and other ions in an aqueous environment, we performed fluorescence and UV-vis titrations in THF–H_2O (3 : 1, v/v). Upon excitation at 370 nm, the spectrum of sensor **1** showed a characteristic emission at 412 nm, attributed to the anthracene emission. Upon gradual addition of Hg^{2+} (up to 7 equiv.) to the solution of compound **1** in THF–H_2O (3 : 1, v/v), an enhancement in the emission, accompanied with a 10 nm red-shift was observed (Fig. 3a). Under the illumination of UV light a bluish colour of the receptor solution containing Hg^{2+} was noticed (inset of Fig. 3a). This was not observed with other metal ions. In the event of other metal ions interacting, the interaction was weak so the change in emission of **1** was almost negligible. The corresponding bar plot in Fig. 3b clearly demonstrates this.

To understand the selectivity in the sensing of Hg^{2+} by **1**, we recorded the emission of **1** upon adding 7 equiv. amounts of Hg^{2+} in the presence and absence of 7 equiv. amounts of other metal ions (Fig. 4a). The pronounced 'off–on' type of Hg^{2+}-selectivity was noticed even in the presence of other metal ions. The plot of the fluorescence ratio in Fig. 4b interprets this aspect.

Simultaneous UV-vis titrations were performed to gain an insight into the binding interaction of **1** in the ground state.

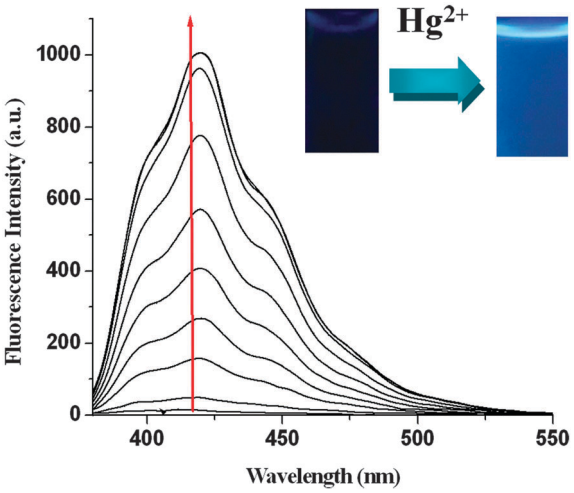

Fig. 1 The change in emission of **1** ($c = 2.5 \times 10^{-5}$ M) in THF upon gradual addition of 1.5 equiv. of $Hg(ClO_4)_2$ ($c = 1.0 \times 10^{-3}$ M). The inset shows the fluorescence colour change under UV irradiation.

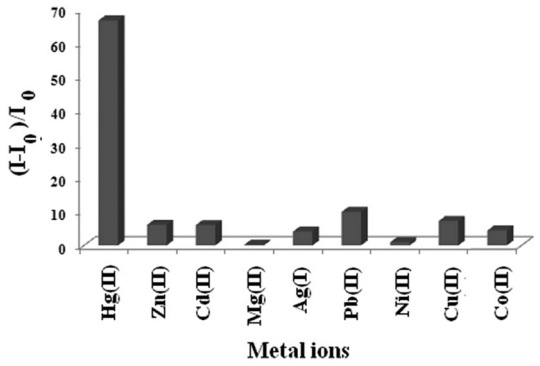

Fig. 2 Fluorescence ratio ($I - I_0/I_0$) of **1** ($c = 2.5 \times 10^{-5}$ M) at 420 nm upon addition of 2 equiv. amounts of particular cations in THF.

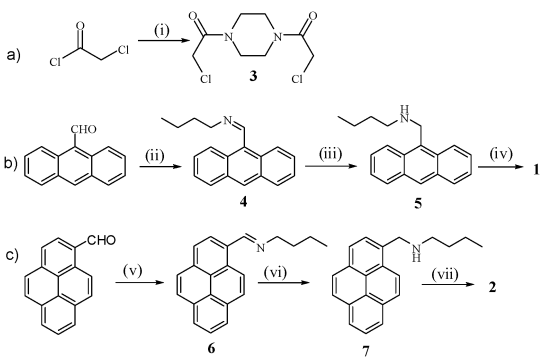

Scheme 2 a) (i) Piperazine, dry Et_3N, dry CH_2Cl_2, stir, 8 h. b) (ii) *n*-Butylamine, dry CH_3OH, reflux, 6 h; (iii) $NaBH_4$, CH_3OH, reflux, 6 h; (iv) **3**, anhydrous K_2CO_3, dry CH_3CN, reflux, 14 h. c) (v) *n*-Butylamine, dry C_6H_6, reflux, 6 h; (vi) $NaBH_4$, CH_3OH, reflux, 6 h; (vii) **3**, anhydrous K_2CO_3, dry CH_3CN, reflux, 14 h.

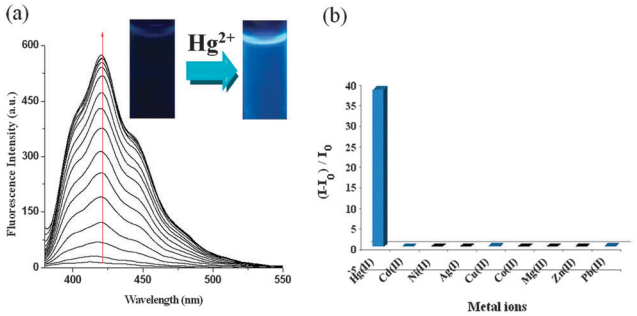

Fig. 3 (a) The change in emission of **1** ($c = 2.5 \times 10^{-5}$ M) in THF–H_2O (3 : 1, v/v) upon gradual addition of 7 equiv. of $Hg(ClO_4)_2$ ($c = 1.0 \times 10^{-3}$ M). The inset shows the fluorescence colour change under UV irradiation. (b) Fluorescence ratio ($I - I_0/I_0$) of **1** ($c = 2.5 \times 10^{-5}$ M) at 420 nm upon addition of 7 equiv. amounts of particular cations in THF–H_2O (3 : 1, v/v).

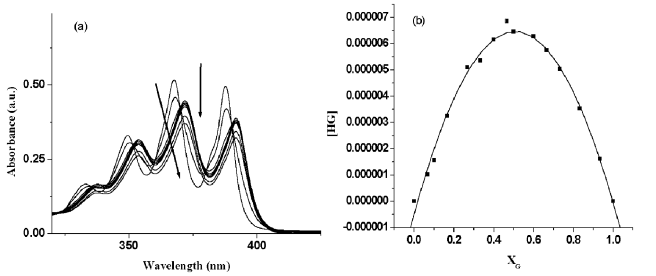

Fig. 5 (a) The change in absorption of **1** ($c = 2.5 \times 10^{-5}$ M) in THF–H_2O (3 : 1, v/v) upon gradual addition of 10 equiv. of $Hg(ClO_4)_2$ ($c = 1.0 \times 10^{-3}$ M). (b) Fluorescent Job's plot of receptor **1** ($c = 2.5 \times 10^{-5}$ M) with Hg^{2+} at 412 nm (λ_{ex} = 370 nm) in THF–H_2O (3 : 1, v/v).

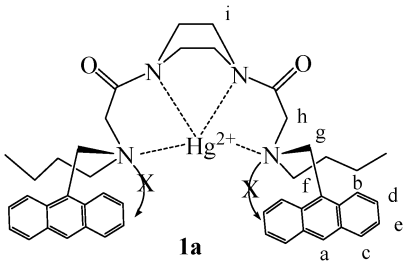

Fig. 6 Probable binding structure of **1** with Hg^{2+}.

The intensity of the absorption peaks at 350 nm, 367 nm and 388 nm for anthracene decreased upon complexation of cations (ESI†). In the presence of Hg^{2+} the change in intensity of anthracene absorption was relatively large compared to the other cations examined. Upon gradual addition of Hg^{2+} the absorption peaks for anthracene underwent a red shift (ESI†). In THF–H_2O (3 : 1, v/v) the decrease in the intensity of the absorption for anthracene upon gradual addition of Hg^{2+} (Fig. 5a) was noted to be less compared to the case in THF.

In the interaction process, sensor **1** gave a 1 : 1 stoichiometry with Hg^{2+} as confirmed by fluorescence (Fig. 5b) as well as UV Job's plots (ESI†).[18] The association constant[19a] of the complex was determined to be $(1.33 \pm 0.31) \times 10^4$ M^{-1} (ESI†). We were unable to determine the binding constant values for the other cations due to minor changes in emission. Based on these findings, a probable mode of binding of Hg^{2+} by **1** is represented in Fig. 6.

The amide group, being a chelator, may coordinate with the metal ion either through the amide nitrogen or the carbonyl oxygen. The involvement of the amide nitrogen in coordination in the present case was confirmed by FTIR. The signal for amide carbonyl stretching appeared at 1643 cm^{-1} and moved to 1650 cm^{-1} upon complexation (ESI†). In addition, the participation of the nitrogen centres in complexation according to the mode shown in Fig. 6 was established by downfield chemical shift of the protons of the adjacent $-CH_2-$ groups in ^1H NMR (Fig. 7). However, during interaction, the anthracene ring protons underwent a small downfield shift thereby suggesting the negligible contribution of cation–π interaction in the binding event.

During interaction, the signals for the protons of types 'a', 'b' and 'c' of the anthracene ring moved downfield by 0.12, 0.03 and 0.03 ppm, respectively. The protons of the methylene groups of types 'g', 'h' and 'f' also underwent downfield shifts by 0.03, 0.23 and 0.20 ppm, respectively. This change in chemical shift of the methylene protons indicated the involvement of the nitrogen centers in complexation. A small downfield

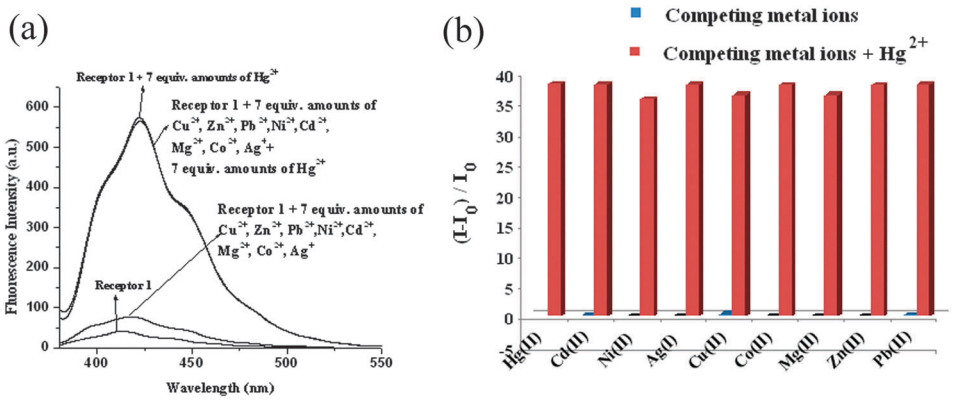

Fig. 4 (a) The change in emission of **1** ($c = 2.5 \times 10^{-5}$ M) in THF–H_2O (3 : 1, v/v) upon addition of 7 equiv. of $Hg(ClO_4)_2$ ($c = 1.0 \times 10^{-3}$ M) in the presence and absence of 7 equiv. of other metal ions. (b) Competitive selectivity of **1** ($c = 2.5 \times 10^{-5}$ M) towards Hg^{2+} in the presence of different cations in THF–H_2O (3 : 1, v/v).

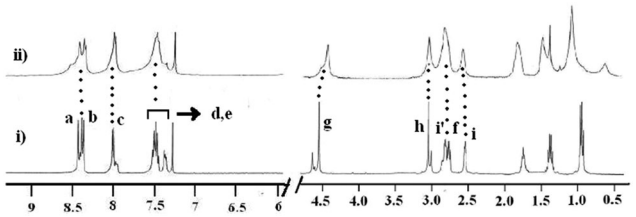

Fig. 7 Partial ^{1}H NMR (400 MHz, $CDCl_3$) of (i) **1** ($c = 1 \times 10^{-3}$ M) and (ii) **1** in the presence of 1 equiv. amount of $Hg(ClO_4)_2$ (see the labeling of the protons of **1** in Fig. 6).

chemical shift (0.01 ppm) of protons of type 'i' of the piperazine unit in the presence of Hg^{2+} ions cannot be ignored from its participation in complexation. However, the absence of excimer emission of **1** in the presence of Hg^{2+} signifies that the appended anthracenes are apart from the distance required for π-stacking either intra or intermolecularly. This information overall supports our proposition in Fig. 6.

Thus, the dimension of the open cavity as well as the coordination abilities of the two pendant arms makes **1** a good host for Hg^{2+}. The fluorometric behaviour of **1** with Hg^{2+} ions was also checked in THF–H_2O (3 : 1, v/v) using HEPES buffer (10 mmol, pH 7.4). Here we noted a similar change and selectivity of **1** towards Hg^{2+} ions (ESI†). It is mentionable that compound **1** was able to detect Hg^{2+} ions at concentrations as low as 3×10^{-4} M (ESI†).

We also synthesized compound **2**, which consists of an identical binding site with pyrene as the signalling probe instead of anthracene. As expected, with the gradual addition of Hg^{2+} ions, receptor **2** also showed an increase in emission at 386 nm and exhibited a 1 : 1 stoichiometry of the complex (ESI†). The increase in emission in the presence of Hg^{2+} ions is attributed to the formation of a complex like the mode shown in Fig. 6 that results in the inhibition of the PET process (ESI†) from the binding site to the excited state of the fluorophore. The binding constant of **2** with Hg^{2+} was calculated[19b] to be 1.32×10^4 M^{-1}. Compound **2** also showed strong selectivity towards Hg^{2+} over other metal ions with a detection limit of 3×10^{-4} M. This observation shows that the change of the aromatic surface in the design has little effect on the binding and selection; rather the chelating centres contribute more to the binding of metal ions.

However, to test the reversibility of binding in such sensors we titrated the Hg^{2+} complex of **1** with biothiols such as cysteine, homocysteine and glutathione, which play important roles in maintaining the appropriate redox status of biological systems.[8] The gradual addition of cysteine and homocysteine up to 30 equiv. to a solution of the mercury complex of **1** in THF–H_2O (3 : 1, v/v; using 10 mmol HEPES buffer, pH 7.4) induced partial quenching of the emission of **1**·Hg^{2+} (ESI†). In contrast, under identical conditions, increasing the addition of reduced glutathione (up to 30 equiv.) to the solution of the **1**·Hg^{2+} complex (Fig. 8) resulted in complete quenching of the emission indicating that Hg^{2+} ions are completely removed from the binding centres. The corresponding plot in Fig. 9

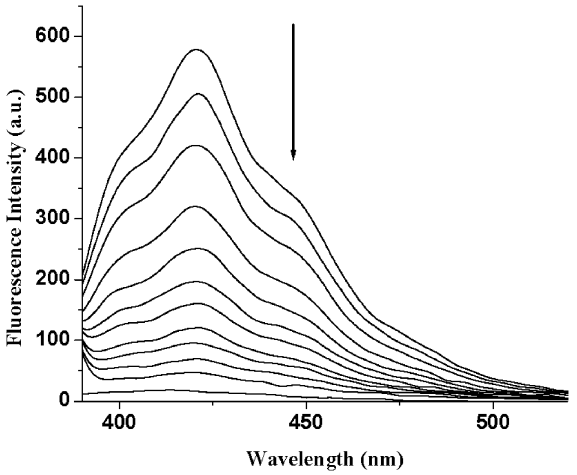

Fig. 8 Emission spectra for the **1**·Hg^{2+} complex upon addition of 30 equiv. amounts of glutathione in THF–H_2O (3 : 1, v/v; 10 mmol HEPES, pH 7.4).

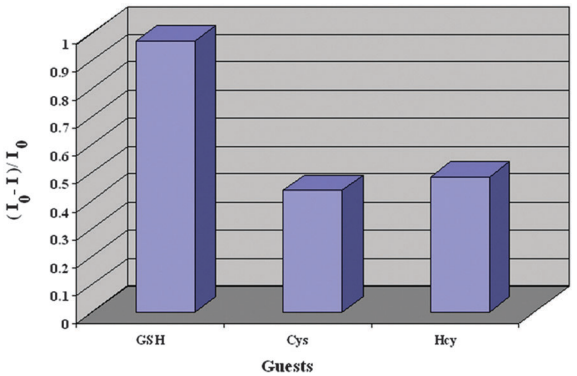

Fig. 9 The change in the fluorescence ratio at 420 nm for the **1**·Hg^{2+} ensemble upon addition of 30 equiv. of various thiols ($c = 1 \times 10^{-3}$ M) in THF–H_2O (3 : 1, v/v; 10 mmol HEPES buffer, pH 7.4; λ_{ex} = 370 nm).

reports the ability of the **1**·Hg^{2+} ensemble to selectively sense GSH over cysteine and homocysteine under physiological conditions.

During interaction of glutathione with the mercury complex of **1** the bluish color of the solution of **1**·Hg^{2+} observed under UV exposure was discharged. Further addition of Hg^{2+} retrieved the color (Fig. 10). The spectral changes, in this aspect, can be found in the ESI†. Thus the overall observations indicate that while compound **1** with simple architecture is excellent to act as a reversible 'off–on' molecular switch for Hg^{2+} ions, the **1**·Hg^{2+} ensemble behaves as an 'on–off' switch to GSH.

A similar finding was not fully achieved with sensor **2** (ESI†). In contrast, the **2**·Hg^{2+} complex showed less selectivity towards GSH as both cysteine and homocysteine resulted in significant quenching of the emission of **2**·Hg^{2+}. Therefore, the 'on–off' switching in the presence of Hg^{2+} and all the biothiols was observed without any distinguishing features (ESI†).

In an effort to construct the molecular logic gate, we investigated the ''off–on'' switching process in **1** by a sequence dependent emission output between these chemical inputs. Herein, the simple molecular system **1** correlates very well with

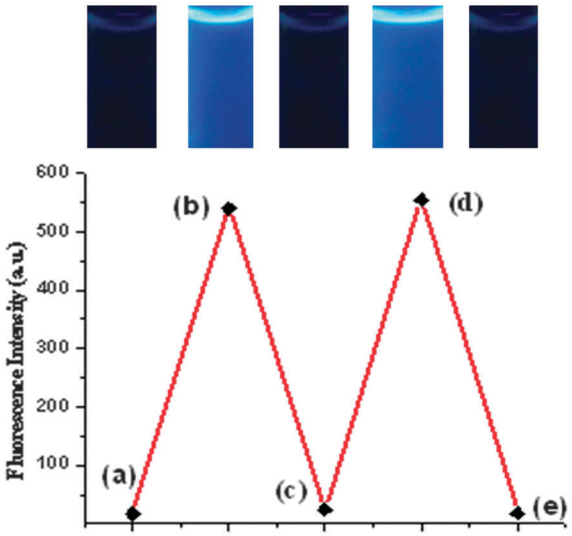

Fig. 10 Fluorescence experiment showing the reversible off–on–off switching for Hg^{2+} and GSH; above are the vials showing the visual fluorescent colour change at every cycle, where a = **1**; b = **1** + Hg^{2+}; c = b + GSH; d = c + Hg^{2+}; e = d + GSH (Hg^{2+} = 14 equiv., GSH = 30 equiv.).

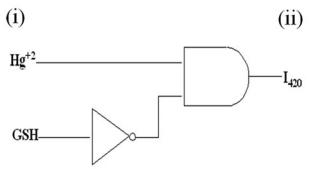

Input		Output
Hg^{2+}	GSH	I_{420}
0	0	0
0	1	0
1	0	1
1	1	0

Fig. 11 (i) The logic circuit of receptor **1** with chemical inputs of Hg^{2+} and GSH, mimicking an INHIBIT gate; (ii) truth table for the INHIBIT gate of **1** with chemical inputs of Hg^{2+} and GSH.

an INHIBIT logic gate. In considering the INHIBIT logic gate properties of **1**, Hg^{2+} and GSH act as inputs while the emission intensity at 420 nm (I_{420}) is the output (Fig. 11i and ii). The output is *zero* and the gate is OFF when (a) both the Hg^{2+} and GSH are absent, (b) GSH alone is present, or (c) both Hg^{2+} and GSH are present. The output is *one* and the gate is ON only when Hg^{2+} alone is present. Thus **1** can act as an INHIBIT logic gate.

Finally, the potentiality of **1** in biological systems was evaluated for *in vitro* detection of Hg^{2+} ions in human cervical cancer (HeLa) cells. The HeLa cells were incubated with 5 μl of sensor **1** (10 μM) in THF–H_2O (3 : 1, v/v) in DMEM (Dulbecco's modified Eagle's medium, without FBS) for 30 min at 37 °C and washed with phosphate buffered saline (PBS, pH = 7.4) to remove excess **1**. DMEM (without FBS) was again added to the cells. The cells were then treated with 5 μl of $Hg(ClO_4)_2$ (30 μM) and incubated again for 30 min at 37 °C. A control set of cells which was devoid of Hg^{2+} ions was kept. The addition of **1** to the cells did not show any cytotoxicity as is evident from the morphology of the cells. Herein, Fig. 12a and b represent the bright field images of the cells before and after treatment of

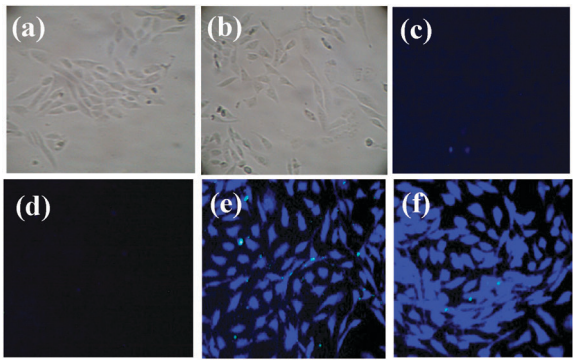

Fig. 12 Fluorescence and bright field images of HeLa cells: (a) bright field image of normal cells, (b) bright field image of cells treated with receptor **1** (10 μM) for 1 h at 37 °C, (c) fluorescence image of cells treated with **1** (10 μM) for 1 h at 37 °C, (d) fluorescence image of cells treated with $Hg(ClO_4)_2$ (30 μM) for 1 h at 37 °C, (e) blue fluorescence images of the cells upon treatment with receptor **1** (10 μM) and then $Hg(ClO_4)_2$ (30 μM) for 30 min at 37 °C, (f) blue fluorescence images of the cells upon treatment with **1** (10 μM) and then $Hg(ClO_4)_2$ (30 μM) for 1 h at 37 °C; λ_{ex} = 370 nm.

the cells with **1**, respectively. Cells incubated with sensor **1** without Hg^{2+} (Fig. 12c) and cells incubated with Hg^{2+} without sensor **1** (Fig. 12d) did not show any fluorescence properties. In contrast, cells incubated with sensor **1** and then with Hg^{2+} ions showed the occurrence of blue fluorescence indicating the permeability of sensor **1** inside the cells as well as the binding of Hg^{2+} with the sensor (Fig. 12e and f).

The glutathione induced reversible "off–on" experiment that could serve as experimental evidence to support the reversible as well as selective sensing of glutathione over cysteine and homocysteine was also applied to human cervical cancer (HeLa) cells. The blue coloured cells obtained from incubation with the receptor followed by treatment with Hg^{2+} showed no fluorescence upon addition of GSH (80 μM) (Fig. 13).

The addition of sensor **1** to the cells did not show any cytotoxicity as is evident from the morphology of the cells (Fig. 12) as well as the MTT assay depicted in the ESI.†[20] The viability was more than 90%, 90% and 91% for normal, acetonitrile and receptor-treated cells, respectively. Since the percentage of viable cells of all the series was above 90% this would suggest that the receptor was not cytotoxic when exposed to cultured cells *in vitro*. The cell permeability and cytotoxicity of **2** were also documented in the same way as was done for **1** and the results were noticed to be nearly identical (ESI†).

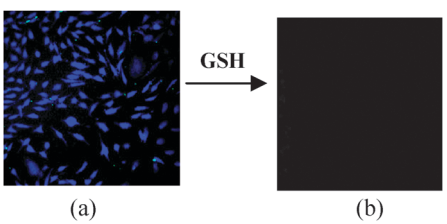

Fig. 13 Fluorescence images of HeLa cells: (a) blue fluorescence images of cells upon treatment with sensor **1** (10 μM) and then $Hg(ClO_4)_2$ (30 μM) after 1 h, (b) fluorescence images of cells upon addition of GSH (80 μM) to the ensemble of **1** (10 μM) and $Hg(ClO_4)_2$ (30 μM) after 1 h.

Conclusion

In conclusion, we have developed the simple and easy-to-make piperazine-based PET sensory systems **1** and **2**, which show excellent responses towards Hg^{2+} ion in semi-aqueous systems by exhibiting increased emission and fluorescence. Furthermore, between **1** and **2**, sensor **1** in its complexed form with Hg^{2+} has been established as a good ensemble to detect glutathione (GSH) over cysteine and homocysteine. Sensor **1** operates as an INHIBIT logic gate when Hg^{2+} and GSH are considered as the possible inputs. In addition, compounds **1** and **2** are both cell permeable and able to detect intracellular Hg^{2+} ions through fluorescence imaging.

Experimental

Syntheses

1,1′-(Piperazine-1,4-diyl(2-chloroethanone)) (3). To a stirred solution of piperazine (1 g, 11.61 mmol) in 40 ml dry CH_2Cl_2, chloroacetyl chloride (2.77 ml, 34.83 mmol) and dry Et_3N (4.850 ml, 34.82 mmol) were added dropwise. The reaction mixture was stirred at room temperature for 8 h. The solvent was evaporated under vacuum. The residue was taken in water (40 mL), and the product was extracted with $CHCl_3$ (3 × 40 mL). The combined organic layer was dried over anhydrous sodium sulphate and evaporated *in vacuo*. The crude product was purified by column chromatography using ethyl acetate–petroleum ether (1 : 1, v/v) as eluent to give the desired product **3** as a pale brown solid (2 g, yield: 72.1%); m.p. 133 °C; ^{1}H NMR (400 MHz, $CDCl_3$): δ 4.10 (s, 4H), 3.72–3.56 (m, 8H); FTIR (KBr, cm^{-1}): 2991, 2908, 2879, 1338.

Anthracen-9-ylmethyl-butyl-amine (5). To a solution of 9-anthranaldehyde (0.4 g, 1.94 mmol) in dry methanol, *n*-butyl amine (0.193 ml, 1.94 mmol) was added and the reaction mixture was refluxed for 6 h. The Schiff base **4** thus formed *in situ* was reduced by refluxing the mixture with $NaBH_4$ (0.150 g, 3.96 mmol) for 6 h. The progress of the reduction was monitored by thin layer chromatography (TLC) (petroleum ether–EtOAc, 80 : 20, v/v). After completion of the reaction, the solvent was evaporated under reduced pressure. Then, $CHCl_3$–water (2 : 1, v/v) was added to the residue and the compound was extracted with $CHCl_3$. The organic phase was dried over anhydrous Na_2SO_4 and evaporated *in vacuo*. The crude product was purified by column-chromatography using petroleum ether–EtOAc, 80 : 20 (v/v) as eluent to afford amine **5** as a yellow gummy product (0.42 g, yield: 82.3%), ^{1}H NMR (400 MHz, $CDCl_3$): δ 8.53 (s, 1H), 8.34 (d, 2H, J = 8 Hz), 8.01 (d, 2H, J = 8 Hz), 7.55 (t, 2H, J = 8 Hz), 7.46 (t, 2H, J = 8 Hz), 4.75 (s, 2H, Ar*CH*$_2$), 2.87 (t, 2H, J = 8 Hz, NH*CH*$_2$), 1.88 (br s, 1H, *NH*), 1.62–1.55 (m, 2H, NHCH$_2$*CH*$_2$), 1.41–1.31 (m, 2H, NHCH$_2$CH$_2$*CH*$_2$), 0.91 (t, 3H, J = 8 Hz, NHCH$_2$CH$_2$CH$_2$*CH*$_3$); FTIR (KBr, cm^{-1}): 3412, 3046, 2953, 2911, 1444.

Butyl-pyren-1-ylmethylene-amine (7). To a solution of pyrene-1-carboxaldehyde (1 g, 4.34 mmol) in dry benzene, *n*-butyl amine (0.474 ml, 0.477 mmol) was added and the reaction mixture was allowed to reflux for 6 h. The Schiff base **6** formed *in situ* was reduced by refluxing the mixture with $NaBH_4$ (0.19885 g, 5.26 mmol) for 6 h. The reaction was quenched by evaporation of the solvent under reduced pressure. $CHCl_3$–water (2 : 1) was added to the residue and the compound was extracted with $CHCl_3$. The organic phase was dried over anhydrous Na_2SO_4 and evaporated *in vacuo*. The crude product was purified by column-chromatography using petroleum ether–EtOAc, 80 : 20 (v/v) as eluent to afford amine **7** as a pale yellow solid (0.910 g, yield: 90.4%), m.p. 95 °C; ^{1}H NMR (400 MHz, $CDCl_3$): δ 8.36 (d, 1H, J = 8 Hz), 8.18–8.11 (m, 4H), 8.03–7.97 (m, 4H), 4.87 (br s, 1H, *NH*), 4.48 (s, 2H, Ar*CH*$_2$), 2.79 (t, 2H, J = 8 Hz, NH*CH*$_2$), 1.60–1.53 (m, 2H, NHCH$_2$*CH*$_2$), 1.42–1.33 (m, 2H, NHCH$_2$CH$_2$*CH*$_2$), 0.92 (t, 3H, J = 8 Hz, NHCH$_2$CH$_2$CH$_2$*CH*$_3$). FTIR (KBr, cm^{-1}): 3400, 2950, 2926, 2858, 2813, 1442.

Receptor 1. To a stirred solution of amine **5** (0.347 g, 1.32 mmol) in 20 ml dry CH_3CN, anhydrous K_2CO_3 (0.3 g, 2.17 mmol) was added and the mixture was stirred for 30 min. Compound **3** (0.15 g, 0.63 mmol) was then added and the reaction mixture was refluxed for 14 h and the progress of the reaction was monitored by TLC. After completion of the reaction CH_3CN was evaporated in a vacuum. $CHCl_3$–water (3 : 1, v/v) was added to the residue and the compound was extracted with $CHCl_3$. The combined organic layer was dried over anhydrous Na_2SO_4 and the solvent was evaporated *in vacuo*. The crude product was purified through column chromatography using 25% EtOAc in petroleum ether as eluent to give the desired receptor **1** as a yellow solid (0.34 g, yield: 78.21%), m.p. 180 °C; ^{1}H NMR (400 MHz, $CDCl_3$): δ 8.41 (s, 2H), 8.36 (d, 4H, J = 8 Hz), 7.99 (d, 4H, J = 8 Hz), 7.49–7.31 (m, 8H), 4.53 (s, 4H), 3.03 (s, 4H, J = 16 Hz), 2.81–2.75 (m, 8H), 2.54–2.51 (m, 4H), 1.74–1.70 (m, 4H), 1.38–1.34 (m, 4H), 0.92 (t, 6H, J = 8 Hz); ^{13}C NMR (100 MHz, $CDCl_3$): δ 169.6, 131.3, 131.2, 129.1, 128.8, 127.9, 125.9, 125.0, 124.4, 56.9, 55.6, 50.3, 44.4, 41.4, 29.1, 20.8, 14.0; FTIR (KBr, cm^{-1}): 2895, 2836, 2862, 2836, 1643; HRMS (TOF MS ES$^+$): $(M + H)^+$ required 693.4169, found 693.4207.

Receptor 2. To a stirred solution of amine **7** (0.700 g, 2.44 mmol) in 25 ml dry CH_3CN, anhydrous K_2CO_3 (0.460 g, 3.32 mmol) was added and the mixture was stirred for 30 min. Compound **3** (0.264 g, 1.11 mmol) was then added and the reaction mixture was refluxed for 14 h. After completion of the reaction, CH_3CN was evaporated in a vacuum. $CHCl_3$–water (3 : 1, v/v) was added to the residue and the compound was extracted with $CHCl_3$. The combined organic layer was dried over anhydrous Na_2SO_4 and the solvent was evaporated *in vacuo*. The crude product was purified through column chromatography using 25% EtOAc in petroleum ether as eluent to give the desired receptor **2** as a white solid (0.68 g, 0.917 mmol) yield 78.2%, m.p. 135 °C; ^{1}H NMR (400 MHz, $CDCl_3$): δ 8.39 (d, 1H, J = 8 Hz), 8.29 (d, 1H, J = 8 Hz), 8.17 (d, 2H, J = 8 Hz), 8.09–8.03 (m, 4H), 8.02–7.99 (m, 3H), 7.97–7.92 (m, 3H), 7.88–7.86 (m, 2H), 7.83 (d, 1H, J = 8 Hz), 7.77 (d, 1H, J = 8 Hz), 4.20 (d, 4H, J = 8 Hz), 3.13 (d, 4H, J = 8 Hz), 2.82–2.78 (m, 4H), 2.67–2.56 (m, 8H), 1.59–1.53 (m, 4H), 1.42–1.21 (m, 4H), 0.89 (t, 6H, J = 8 Hz); ^{13}C NMR (100 MHz, $CDCl_3$): δ 169.5, 131.4, 131.2, 129.8, 128.7, 127.4, 127.3, 127.0, 126.0 (2C unresolved), 125.4,

125.3 (2C unresolved), 124.9, 124.6, 124.3, 123.5, 57.3, 55.2, 44.7, 41.6, 29.7, 29.0, 20.7, 14.0; FTIR (KBr, cm^{-1}): 2952, 2898, 2822, 2800, 1644; HRMS (TOF MS ES^+): $(M + H)^+$ required 741.4169, found 741.7592.

General procedure for fluorescence and UV-vis titrations

Stock solutions of the receptors were prepared in THF and 3 : 1 (v/v) THF–H_2O in the concentration range of $\sim 10^{-5}$ M. 2 ml of the receptor solution was taken in the cuvette. Stock solutions of guests in the concentration range of $\sim 10^{-4}$ M, were prepared in the same solvents and were individually added in different amounts to the receptor solution. Upon addition of metal ions, the change in emission of the receptor was noted. The same stock solutions of receptors and guests were used to perform the UV-vis titration experiment. The solutions of the metal salts were successively added in different amounts to the receptor solution (2 mL) taken in the cuvette and the absorption spectra were recorded. Both fluorescence and UV-vis titration experiments were carried out at 25 °C.

Job plots

The stoichiometry was determined by the continuous variation method (Job plot).[18] In this method, solutions of host and guests of equal concentrations were prepared in the solvents used in the experiment. Then host and guest solutions were mixed in different proportions maintaining a total volume of 3 mL of the mixture. All the prepared solutions were kept for 1 h with occasional shaking at room temperature. Then emission and absorbance of the solutions of different compositions were recorded. The concentration of the complex *i.e.*, [HG] was calculated using the equation $[HG] = \Delta I/I_0 \times [H]$ or $[HG] = \Delta A/A_0 \times [H]$ where $\Delta I/I_0$ and $\Delta A/A_0$ indicate the relative emission and absorbance intensities, respectively. [H] corresponds the concentration of pure host. The mole fraction of the host (X_H) was plotted against the concentration of the complex [HG]. In the plot, the mole fraction of the host at which the concentration of the host–guest complex [HG] is maximum gives the stoichiometry of the complex.

Method for the MTT assay

Reagents. MTT [3-(4,5-dimethyl-thiazol-2-yl)-2,*S*-diphenyl-tetrazolium bromide], and DMSO were purchased from Sigma-Aldrich Inc. (St-Louis, MO, USA); Dulbecco's modified Eagle's medium (DMEM), fetal bovine serum, and antibiotics, namely, penicillin, streptomycin, and neomycin (PSN) were purchased from Gibco BRL (Grand Island, NY, USA). All organic solvents used were of high performance liquid chromatography grade.

Cell culture. Cells of the human cervical cancer cell line HeLa were procured from the National Centre for Cell Science, Pune, India. 5×10^5 cells per mL were cultured in DMEM supplemented with 10% fetal bovine serum and 1% PSN antibiotic at 37 °C with a constant supply of 5% CO_2.

Assessment of the percentage of viable cells. The percentage viability of the HeLa cells, after being exposed to both the receptors, was evaluated by the MTT assay (Mossman, 1983). The cells were incubated in 96-well microplates for 24 hours along with the receptors at different concentrations. A set of HeLa cells not exposed to any of the receptors were kept as an untreated control. Other sets of cells were incubated with receptor **1** through 5 μl of stock solution. The cells were allowed to grow for the next 24 hours. MTT was then added to each well and incubated for the next 4 h. The intracellular formazan crystals formed were solubilized with dimethyl sulfoxide (DMSO) and the absorbance of the solution was measured at 595 nm by using a microplate reader (Thermo scientific, Multiskan ELISA, USA). The percentage of cell survival was calculated as: (mean experimental absorbance/mean control absorbance) ×100%.

Acknowledgements

We thank DST and UGC, New Delhi, India for providing facilities in the department. DT thanks CSIR, New Delhi, India for a fellowship.

References

1 (*a*) A. W. Czarnik, *Fluorescent Chemosensors for Ions and Molecule Recognition*, American Chemical Society, Washington, D. C., 1992; (*b*) A. P. de Silva, D. B. Fox, A. J. M. Huxley and T. S. Moody, *Coord. Chem. Rev.*, 2000, **205**, 41; (*c*) X. He, H. Liu, Y. Li, S. Wang, Y. Li, N. wang, J. Xiao, X. Xu and D. Zhu, *Adv. Mater.*, 2005, **17**, 2811; (*d*) D. T. Quang and J. S. Kim, *Chem. Rev.*, 2007, **107**, 3780; (*e*) A. W. Czarnik, *Acc. Chem. Res.*, 1994, **27**, 302.

2 (*a*) V. Amendola, L. Fabbrizzi, M. Licchelli, C. Mangano and P. Pallavicini, *Acc. Chem. Res.*, 2001, **34**, 488; (*b*) E. M. Nolan and S. J. Lippard, *Acc. Chem. Res.*, 2009, **42**, 193; (*c*) G. Muthaup, A. Schlicksupp, L. Hess, L. D. Beher, T. Ruppert, C. L. Masters and K. Beyreuther, *Science*, 1996, **271**, 1406; (*d*) R. A. Løvstad, *Biometals*, 2004, **17**, 111; (*e*) D. G. Barceloux and D. Barceloux, *J. Toxicol., Clin. Toxicol.*, 1999, **37**, 217; (*f*) B. Sarkar, in *Metal ions in biological systems*, ed. H. Siegel and A. Siegel, Marcel Dekker, New York, 1981, vol. 12, p. 233; (*g*) E. L. Que, D. W. Domaille and C. J. Chang, *Chem. Rev.*, 2008, **108**, 1517.

3 (*a*) G. E. Mckeown-Eyssen, J. Ruedy and A. Neims, *Am. J. Epidemol.*, 1983, **118**, 470; (*b*) P. W. Davidson, G. J. Myers, C. Cox, C. F. Shamlaye, D. O. Marsh, M. A. Tanner, M. Berlin, J. Sloane-Reeves, E. Cernichiari, O. Choisy, A. Choi and T. W. Clarkson, *Neurotoxicology*, 1995, **16**, 677; (*c*) P. Grandjean, P. Weihe, R. F. White and F. Debes, *Environ. Res.*, 1998, **77**, 165; (*d*) Z. Zhang, D. Wu, X. Guo, X. Qian, Z. Lu, Q. Zu, Y. Yang, L. Duan, Y. He and Z. Feng, *Chem. Res. Toxicol.*, 2005, **18**, 1814; (*e*) P. Grandjean, P. Weihe, R. F. White and F. Debes, *Environ. Res.*, 1998, **77**, 165.

4 Fluorescent receptors for Hg^{2+} ions: (*a*) M. Yuan, Y. Li, J. Li, C. Li, X. Liu, J. Lv, J. Xu, H. Liu, S. Wang and D. Zhu, *Org. Lett.*, 2007, **9**, 2313; (*b*) M. Zhu, M. Yuan, X. Liu, J. Xu, J. Lv, C. Huang, H. Liu, Y. Li, S. Wang and D. Zhu, *Org. Lett.*, 2004,

6, 1489; (*c*) H.-K. Chen, C.-Y. Lu, H.-J. Cheng, S.-J. Chen, C.-H. Hu and A.-T. Wu, *Carbohydr. Res.*, 2010, **345**, 2557; (*d*) J. Hu, M. Zhang, B. L. Yu and Y. Ju, *Bioorg. Med. Chem. Lett.*, 2010, **20**, 4342; (*e*) A. Thakur, S. Sardar and S. Ghosh, *Inorg. Chem.*, 2011, **50**, 7066; (*f*) S.-M. Cheung and W.-H. Chan, *Tetrahedron*, 2006, **62**, 8379; (*g*) H. N. Kim, M. H. Lee, H. J. Kim, J. S. Kim and J. Yoon, *Chem. Soc. Rev.*, 2008, **37**, 1465; (*h*) A. Cabellero, A. Espinosa, A. Tarraga and P. Molina, *J. Org. Chem.*, 2008, **73**, 5489; (*i*) J. Wang and B. Liu, *Chem. Commun.*, 2008, 4759; (*j*) Y. Zhao, B. Zheng, J. Du, D. Xiao and L. Yang, *Talanta*, 2011, **85**, 2194; (*k*) J. S. Kim, S. Y. Lee, J. Yoon and J. Vicens, *Chem. Commun.*, 2009, 4791.

5 (*a*) G.-Q. Shang, X. Gao, M.-X. Chen, H. Zheng and J.-G. Xu, *J. Fluoresc.*, 2008, **18**, 1187; (*b*) H. Liu, P. Yu, D. Du, C. He, B. Qiu, X. Chen and G. Chen, *Talanta*, 2010, **81**, 433; (*c*) G. He, X. Zhang, C. He, X. Zhao and C. Duan, *Tetrahedron*, 2010, **66**, 9762; (*d*) S. Atilgan, I. Kutuk and T. Ozdemir, *Tetrahedron Lett.*, 2010, **51**, 892; (*e*) K. Ghosh, T. Sarkar and A. Samadder, *Org. Biomol. Chem.*, 2012, **10**, 3236.

6 A. P. de Silva, H. Q. N. Gunaratne, T. Gunnlaugsson, A. J. M. Huxley, C. P. McCoy, J. T. Rademacher and T. E. Rice, *Chem. Rev.*, 1997, **97**, 1515.

7 D. S. McClure, *J. Chem. Phys.*, 1952, **20**, 682.

8 (*a*) E. M. Nolan and S. J. Lippard, *J. Am. Chem. Soc.*, 2007, **129**, 5910; (*b*) G. He, Y. Zhao, C. He, Y. Liu and C. Duan, *Inorg. Chem.*, 2008, **47**, 5169; (*c*) B. Liu and H. Tian, *Chem. Commun.*, 2005, 3156; (*d*) A. Coskun and E. U. Akkaya, *J. Am. Chem. Soc.*, 2006, **128**, 14474; (*e*) Z. J. Lu, P. N. Wang, Y. Zhang, J. Y. Chen, S. Zhen, B. Leng and H. Tian, *Anal. Chim. Acta*, 2007, **597**, 306; (*f*) H. Zhang, Q. L. Wang and Y. B. Jiang, *Tetrahedron Lett.*, 2007, **48**, 3959; (*g*) J. B. Wang and X. H. Qian, *Chem. Commun.*, 2006, 109; (*h*) F. Guo, X. H. Qian and L. H. Jia, *J. Am. Chem. Soc.*, 2004, **126**, 2272; (*i*) J. Wang, X. Qian and J. Cui, *J. Org. Chem.*, 2006, **71**, 4308; (*j*) H. Zhang, L. F. Han, K. Zachariasse and Y. B. Jiang, *Org. Lett.*, 2005, **7**, 4217.

9 (*a*) D. P. Murale, H. Kim, W. S. Choi and D. G. Churchill, *Org. Lett.*, 2013, **15**, 3630 and references cited therein; (*b*) D. P. Murale, H. Kim, W. S. Choi and D. G. Churchill, *Org. Lett.*, 2013, **15**, 3946; (*c*) B. Zhu, Y. Zhao, Q. Zhou, B. Zhang, L. Liu, B. Du and X. Zhang, *Eur. J. Org. Chem.*, 2013, 888.

10 I. Rahman and W. MacNee, *Free Radical Biol. Med.*, 2000, **28**, 1405.

11 (*a*) X. F. Wang and M. S. Cynader, *J. Neurosci.*, 2001, **21**, 3322; (*b*) J. Liu, H. C. Yeo, E. Overvik-Douki, T. Hagen, S. J. Doniger, D. W. Chu, G. A. Brook and B. N. Ames, *J. Appl. Physiol.*, 2000, **89**, 21.

12 J. C. Ndamanisha, J. Bai, B. Qi and L. Guo, *Anal. Biochem.*, 2009, **386**, 79.

13 (*a*) C. Lu, Y. Zu and V. W. W. Yam, *J. Chromatogr., A*, 2007, **1163**, 328; (*b*) J. Vacek, B. Klejdus, J. Petrlova, L. Lojkova and V. Kuban, *Analyst*, 2006, **131**, 1167.

14 Y. Iwasaki, M. Hoshi, R. Ito, K. Saito and H. Nakazawa, *J. Chromatogr., B: Anal. Technol. Biomed. Life Sci.*, 2006, **839**, 74.

15 Fluorescent receptors for glutathione: (*a*) J. Zhao, C. Chen, L. Zhang, J. Jiang, G. Shen and R. Yu, *Analyst*, 2013, **138**, 1713; (*b*) Y. Xu, B. Li, P. Han, S. Sun and Y. Pang, *Analyst*, 2013, **138**, 1004; (*c*) B. K. McMahon and T. Gunnlaugsson, *J. Am. Chem. Soc.*, 2012, **134**, 10725; (*d*) R. K. Pathak., V. K. Hinge, M. Modal and C. P. Rao, *J. Org. Chem.*, 2011, **76**, 10039; (*e*) N. Shao, J. Jin, H. Wang, J. Zheng, R. Yang, W. Chan and Z. Abliz, *J. Am. Chem. Soc.*, 2010, **132**, 725; (*f*) L.-Y. Niu, Y.-S. Guan, Y.-Z. Chen, L.-Z. Wu, C.-H. Tung and Q.-Z. Yang, *J. Am. Chem. Soc.*, 2012, **134**, 18928 and references cited therein.

16 S. Timur, D. Odaci, A. Dincer, F. Zihnioglu and A. Telefoncu, *Talanta*, 2008, **74**, 1492.

17 D. G. Churchill, *J. Chem. Educ.*, 2006, **83**, 1798.

18 P. Job, *Ann. Chim.*, 1928, **9**, 113.

19 (*a*) B. Valeur, J. Pouget, J. Bourson, M. Kaschke and N. P. Eensting, *J. Phys. Chem.*, 1992, **96**, 6545; (*b*) P. T. Chou, G. R. Wu, C. Y. Wei, C. C. Cheng, C. P. Chang and F. T. J. Hung, *J. Phys. Chem. B*, 2000, **104**, 7818.

20 T. Mossman, *J. Immunol. Methods*, 1983, **65**, 55.